

ENHANCEMENT METHOD OF POWER QUALITY IN MICROGRID

K. Divya Teja*

D. Chinna Kullay Reddy**

*PG Scholar, Dept. of Electrical and Electronic Engineering, Madanapalle Institute of Technology and Science, Madanapalle, India. divyatejareddy.kokatam.01@gmail.com

**Dept. of Electrical and Electronic Engineering, Madanapalle Institute of Technology and Science, Madanapalle, India. dkullayreddy@gmail.com

Abstract: *Distributed Energy Resources (DERs) has been emerging as a promising option to meet the growing customer electrical needs. It has an emphasis on reliabilities and environmentally friendly system. In this scenario, in order to maximize the operation efficiency of the DERs effective integration is needed. It enhances the local customer power supply reliability, system performance and minimizes the system losses. Nowadays with increasing demand on a day to day life microgrid plays a vital role in electricity generation using renewable energy resources. A microgrid usually consists of multiple DERs interfaced to the system through power electronic devices. Usage of power electronic devices in microgrid results in the harmonic generation and leads to various power Quality issues. The main objective in a microgrid is to provide the quality of power to its interconnected inhabitants. In order to overcome harmonic high penetration, frequent voltage fluctuations and over current, a magnetic flux control based variable reactor is proposed. The performance of the variable reactor and integrated power quality controller (IPQC) can be designed and verified by using MATLAB/SIMULINK*

Key words: *Microgrid, power quality, variable reactor, integration ,IPQC*

1. Introduction

In recent years there has been an emerging interest in distributed energy resources moving far from massively centralized power generation.

Distributed energy resources such as Solar power generation & wind energy conversion system [WECS] provides many advantages, particularly as a peaking power supply. The necessity for energy isn't ending. This is often definitely true of electricity that perhaps a massive part of entire world energy consumption. However growing in tandem with energy wants are the considerations regarding sustainable development & environmental problems, like the movement to reduce greenhouse emission emissions.

A microgrid is a portion of the power system that includes interconnected loads distributed generation and energy storage satisfies its own load's demand from native generating sources that helps in reducing the demand on the conventional grid and its greater flexibility. [2] It can be operated in equivalent with the main grid or in islanding mode and has the capacity to supply an extremely reliable system and additionally has the strength to recover quickly from the grid disturbances.

Microgrid ought to be strong in controlling the voltage & frequency and should protect the network and equipment connected to that. The vital aspects of the main electricity grid are efficiency and reliableness that are increased by introducing the micro-grid idea. A microgrid is made by using solar PV or the wind or hybrid generation system.

PV based microgrid must be economical and gives reliable power once it is interconnected with the main grid or when operated in island mode. To extract the maximum power from the PV & WECS, maximum power point tracking (MPPT) techniques were employed with in the system. To design proper MPPT controller, the data concerning the PV module's maximum power at MPP beneath variable environmental conditions like irradiation and temperature is required. The RES will bring new challenges once it is interfaced to the power grid.

However, the generated power from the renewable energy source is often unsteady due to environmental condition. In the same manner, fluctuating nature of the wind causes many power quality issues when wind power is injected into the main grid. The combination of wind energy and solar energy into grid presents technical challenges which need consideration of voltage regulation, stability, power quality issues. Operations of a distribution and transmission network were greatly affecting the power quality.

Voltage sag, Voltage swell, Harmonic distortions, Noise, Voltage fluctuations, Voltage unbalances etc. are the Power quality problems and is of great importance. There has been an intensive growth and fast development within the exploitation of wind energy and solar energy at present. The major issues within the microgrid operation are reliableness, stability, congestion management, power flow management, power quality, protection system and incorporation of additional distributed generators (DGs).

The technical challenges of the microgrid are power flow management between generation side and distributed load side and power quality problem that arises because of PE controllers. Prediction of power generation from the RES may be a tough task because the supply of them varies in step with the environmental conditions. The microgrid wants protection and stable operation once it is operated in both grid connected mode and autonomous mode.

the foremost relevant challenges in microgrid protection and control includes Bidirectional power flow, stability issues, uncertainty. Until now, relevant researches on microgrid power quality controllers are divided into two types: Unifunctional controllers and multifunctional controllers. Unifunctional power quality controllers aim at a definite power quality issue within the microgrid. Harmonic mitigation is primarily investigated.

Managing power flow of microgrid is mostly analyzed. Voltage fluctuation is primarily involved. The overvoltage & over current issue is that the main concern. power quality controller and the grid are combined through a special control theme or topology by multi-functional power quality controllers. However, these multifunctional power quality controllers do not take into consideration most of the above-mentioned prime features of a microgrid.

Till date, there is less research on integrated power quality controller (IPQC) notably ideal for microgrid with above-named options. Also, the microgrid capability is relatively small and it's not reasonable to line up numerous sorts of power quality controller. so as to provide to the peculiar needs of microgrid of harmonic high penetration, frequent voltage fluctuation and overcorrect phenomenon, bi-directional power flow and little capability, variable reactor based integrated power quality controller ideal for microgrid is proposed.

The integrated power quality controller comprises of special qualities like mitigating the harmonic penetration, limiting the fault current controlling the bidirectional power flow and compensating the voltage fluctuation and being absolutely a variable reactor.

2. Principle Of Variable Reactor

2.1. System Configuration

Fig.1 shows the single-phase system configuration of magnetic flux control (MFC) based variable reactor. The turns ratio of transformers primary and secondary coil is depicted by $k=N_1/N_2$. A transformer with an air gap is preferred and its primary winding AX is associated in series or parallel with the power utility. The secondary winding ax isn't connected with a traditional load, however, a voltage supply electrical converter.

The voltages of the first and coil are u_1 and u_2 , severally. Transformers primary winding current i_1 is detected and acts as the reference signal i_{ref} . current sensor gain is denoted by h , DC side of the inverter voltage is U_d , the capacitance of the DC capacitor is C_d . a is governable parameter, which is explained later. The voltage sourced inverter and current management are applied to obtain a controlled current i_2 that has a similar frequency as i_1 . i_2 is reciprocally injected to the secondary winding ax in phase

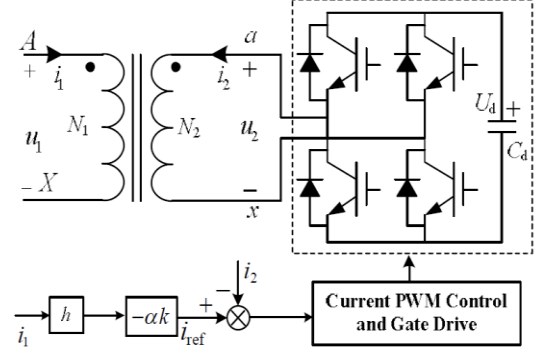


Fig. 1. System configuration of variable reactor

2.2. Equivalent T-Circuit Of Transformer

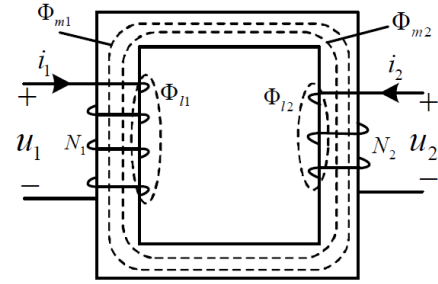


Fig. 2. Magnetically coupled circuit of transformer

The magnetically coupled transformer circuit is central to the variable reactor's operation that is shown in Fig.2. The flow of currents within the two windings produces magneto-motive forces (MMF) which successively create the fluxes.

The total flux linking each winding is expressed as

$$\Phi_1 = \Phi_{l1} + \Phi_{m1} + \Phi_{m2} = \Phi_{l1} + \Phi_m \quad (1)$$

$$\Phi_2 = \Phi_{l2} + \Phi_{m2} + \Phi_{m1} = \Phi_{l2} + \Phi_m \quad (2)$$

Herein Φ_{l1} and Φ_{l2} are the leakage fluxes of primary and secondary windings. The turns of the primary and secondary windings are linked by magnetizing flux Φ_{m1} that is created by primary winding. The turns of primary and secondary windings are linked by the magnetizing flux Φ_{m2} that is created by secondary winding.

The resultant mutual flux denoted by F_m . The transformer voltage equations can be expressed as [15]-[16]

$$u_1 = r_1 i_1 + d\lambda_1/dt \quad (3)$$

$$u_2 = r_2 i_2 + d\lambda_2/dt \quad (4)$$

the resistances of primary and secondary winding are r_1 & r_2 respectively. flux linkages associated with primary and secondary windings are λ_1 and λ_2 respectively. If the system is linear and saturation is neglected, the subsequent equations are often achieved.

$$\lambda_1 = L_{l1} i_1 + L_{m1} (i_1 + \frac{N_2}{N_1} i_2) \quad (5)$$

$$\lambda_2 = L_{l2} i_2 + L_{m2} (\frac{N_1}{N_2} i_1 + i_2) \quad (6)$$

Herein, L_{l1} and L_{l2} are the leakage inductances of primary & secondary winding, respectively. L_{m1} and L_{m2} are the magnetizing inductances of the primary & secondary windings, respectively. $L_{m1} / N_1^2 = L_{m2} / N_2^2$. According to [15]-[16], the quantities of the secondary winding are referred to the primary winding, (3) and (4) become

$$u_1 = r_1 i_1 + L_{l1} \frac{di_1}{dt} + L_{m1} \frac{d}{dt}(i_1 + i_2') \quad (7)$$

$$u_2' = r_2' i_2' + L_{l2}' \frac{di_2'}{dt} + L_{m1} \frac{d}{dt}(i_1 + i_2') \quad (8)$$

In the above equations suffix resembles quantities of secondary winding to primary winding. Equations (7) and (8) is represented as following equations in phasor form

$$U_1 = r_1 I_1 + j\omega L_{l1} I_1 + j\omega L_{m1} (I_1 + I_2') \quad (9)$$

$$U_2' = r_2' I_2' + j\omega L_{l2}' I_2' + j\omega L_{m1} (I_1 + I_2') \quad (10)$$

The voltage equations in (9) and (10) with the common L_{m1} recommend the equivalent T-circuit shown in Fig. 3 for the two-winding transformer.

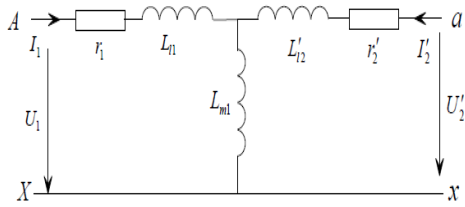


Fig. 3. Equivalent T-circuit of transformer

In some equivalent T-circuit transformers, a core loss resistance r_m , that happens for the core loss as a result of the resultant mutual flux, is interlinked in parallel or series with the magnetizing inductance L_{m1} (a series core-loss resistance r_m is taken into consideration later inside the equivalent T-circuit of the transformer).

Let $Z_1' = r_1' + j\omega L_{l1}'$, which is the outflow impedance of the winding. $Z_2' = r_2' + j\omega L_{l2}'$, which is that the leakage impedance of the secondary winding ax referred to the primary winding. the magnetizing impedance of the transformer $Z_m = r_m + j\omega L_{m1}$. Here, the fundamental angular frequency is ω . And then (9) and (10) become

$$U_1 = Z_1 I_1 + Z_m (I_1 + I_2') \quad (11)$$

$$U_2' = Z_1 I_1 + Z_m (I_1 + I_2') \quad (12)$$

2.3 Principle Of Variable Reactor

In Fig.1, the primary winding current is detected and functions as the reference signal and the voltage source inverter are applied to trace the reference signal so as to yield a controlled current i_2 . When controlled current i_2 and the primary current i_1 satisfy

$$I_2' = -\alpha I_1 \quad (\text{i.e., } I_2 = -\alpha k I_1) \quad (13)$$

Herein, α is a controllable parameter.[1] The transformer is double side energized and then the following equations can be attained.

$$U_1 = Z_1 I_1 + (1 - \alpha) Z_m I_1 \quad (14)$$

$$U_2' = Z_2' I_2' + (1 - 1/\alpha) Z_m I_2' \quad (15)$$

In terms of (14), from the terminals AX, the transformer's equivalent impedance can be obtained.

$$Z_{AX} = U_1 / I_1 = Z_1 + (1 - \alpha) Z_m \quad (16)$$

Using (16), the equivalent impedance of the primary winding of the transformer is the function of the controllable parameter α . primary winding exhibits When α is adjusted, the consecutively adjustable impedance.

The equation (16) may be achieved in the resultant magneto-motive forces of the two windings acting around the same path of the core. voltage source inverter produces a controlled current i_2 is injected into the secondary winding of the transformer and $i_2 = -\alpha k i_1$, the resultant MMF is $N_1 I_1 + N_2 I_2 = (1 - \alpha) N_1 I_1$. Then, the resultant flux created by MMF of the two windings produces the resultant flux is $(1 - \alpha) \Phi_m$. And then, the induced voltage made by the resultant flux may be expressed in phasor form as

$$E_1 = (1 - \alpha) j\omega L_{m1} I_1 \quad (17)$$

The primary voltage equation is often achieved as (14) In terms of (16), the relation between the parameter α & the equivalent impedance of the primary winding is given in TABLE 1.

The variable reactor consists of the following features hardly producing harmonics, simple management situation and with consecutive adjustable impedance. Several FACTS devices will be enforced in terms of the principle. the variable reactor will be utilized in UPFC to vary the line impedance between the sending & receiving ends thus as to control the power flow; it may also substitute the thyristor controlled reactor of TCSC, however, the proposed variable reactor doesn't produce any harmonics; FCL can even be enforced in terms of the principle [16]. the variable reactor. Reactive power compensation all will be realized by the variable reactor.

2.4 Dynamic Analysis Of Variable Reactor

current control is One of the major techniques of the variable reactor based on the magnetic flux control. today the wide used current management Fourier includes the hysteresis current control, the ramp comparison current control and predictive and deadbeat control [11]. within the digital control system based on DSP, the foremost wide used current management is that the ramp comparison current management with PI controller. during this case, the

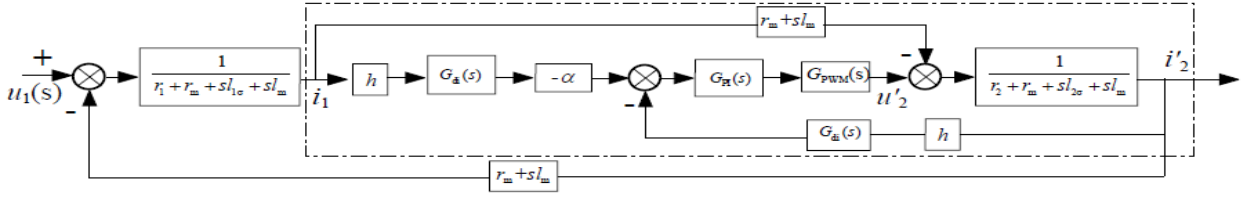


Fig. 4. System block diagram of variable reactor

$$G_Y(S) = i_l(s)/u_l(s) = \frac{hk_1(1+T_1s)K_{PWM} + (r_2+r_m+sI_{2\sigma}+sI_m)(1+T_{di}s)T_1(1+T_{PWM}s)}{hk_1(1+T_1s)K_{PWM}[r_1+r_m+sI_{1\sigma}+sI_m - \alpha(r_m+sI_m)] + [(r_1+sI_{1\sigma})(r_2+sI_{2\sigma}) + (r_m+sI_m)(r_1+r_2+sI_{1\sigma}+sI_{2\sigma})](1+T_{di}s)T_1(1+T_{PWM}s)} \quad (18)$$

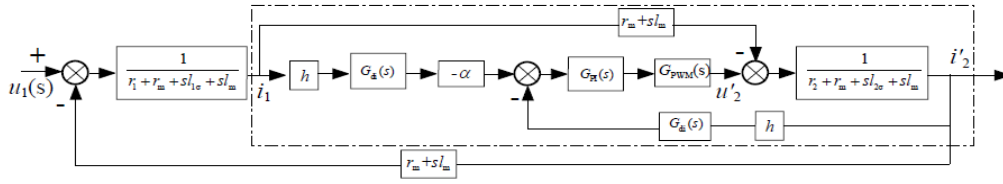


Fig. 5 block diagram of current control with feed forward

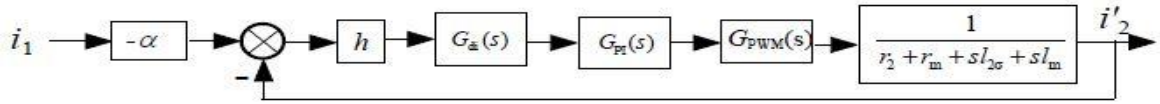


Fig. 6 Structure of current control

block diagram of variable reactor system is shown in Fig. 4.

Table 1. Equivalent Impedance of Primary Winding of Transformer

α	The equivalent impedance of terminal AX	Impedance characteristic
$\alpha < 0$	$Z_{AX} > Z_1 + Z_m$	resistive and inductive
$\alpha = 0$	$Z_{AX} = Z_1 + Z_m$	
$0 < \alpha < 1$	$Z_1 < Z_{AX} < Z_1 + Z_m$	
$\alpha = 1$	$Z_{AX} = Z_1$	0
$1 < \alpha < 1 + Z_1/Z_m$	$Z_1 < Z_{AX} < 0$	
$\alpha = 1 + Z_1/Z_m$	$Z_{AX} = 0$	
$\alpha > 1 + Z_1/Z_m$	$Z_{AX} < 0$	Resistive and capacitive

Herein, h is a gain of current sensor, the combined transfer function of the sample and delay is described as $G_{di}(s) = 1/(1+sT_{di})$, the transfer function of the voltage sourced inverter is denoted $G_{PWM}(s) = K_{PWM}/(1+sT_{PWM})$. The transfer function of the PI controller

is denoted as $G_{PI}(s) = k_i(1+sT_i)/sT_i$. The system admittance transfer function are often derived as (18) ((18) is below Fig. 4), which suggests the system can be a five order system.

the current control component is in dash-dotted frame shown in Fig.4. To boost the system anti-interference performance in low-frequency band, a feed forward element is intended within the block diagram of current control component, that is shown in Fig.5. during this case, the block diagram of current control component becomes Fig. 6.

The open-loop transfer function of current control block in Fig.6

$$G_{open}(s) = \frac{hk_1(1+sT_1)K_{PWM}}{(1+T_{di}s)sT_i(1+T_{PWM}s)(r_2+r_m+sI_{2\sigma}+sI_m)} \quad (19)$$

Let $T_i = (I_{2\sigma} + I_m)/(r_2 + r_m)$ and $T_{PWM} \approx 0.5T_{di}$, once combining the two components with little time delay, (16) becomes

$$G_{open}(s) = \frac{hK_{PWM}T_i/(r_2+r_m)}{(1+1.5T_{di}s)T_i} \quad (20)$$

Here, when $ki = T_i(r_2+r_m)/(3T_{di}K_{PWM}h)$, this control system performance are approximately optimum[26]

2.4. DC-Link Voltage Control Of Variable Reactor

There should be some losses when the variable reactor system with inverter operates usually and the inverter can suck up active power to keep up the DC voltage constant. Fig.7 shows the dc-link voltage control schematic diagram of the variable reactor system. Herein, U_d^* and U_d represent the inverter DC reference and sensible voltage, respectively.

An active current reference i_p is combined to the reference signal i_{ref1} to accomplish a new reference signal i_{ref2} . to create inverter DC practical voltage A dc-link voltage PI controller is applied, U_d follow the DC reference voltage U_d^* . The output of voltage PI controller is multiplied by the phase-lock-loop output of u_2 to yield the active current reference i_p

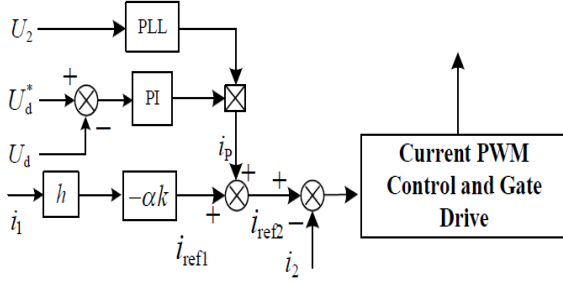


Fig. 7. DC-link voltage control schematic diagram

3.Principle Of Power Quality Controller

3.1. System Configuration

The integrated power quality controller is often equipped in series and parallel in micro grid or point of common couplings (PCC). For simplicity, the IPQC is installed at PCC. Fig.8 shows the three-phase detailed system configuration of the integrated power quality controller with transformer and inverter. the source voltage and impedance of conventional power supply are represented by u_s and L_s , respectively. The passive filters, which have the function of diminishing the harmonics, are shunted on either side. The primary winding of a transformer is inserted in series between the microgrid and the conventional power utility, while the secondary winding is inter-connected with a voltage-source PWM converter. U_d is that the voltage of DC side of the inverter. The microgrid contains a harmonic load, a solar cell system, Wind energy conversion system, battery storage system and a normal load. The proposed integrated power quality controller has the following functions.

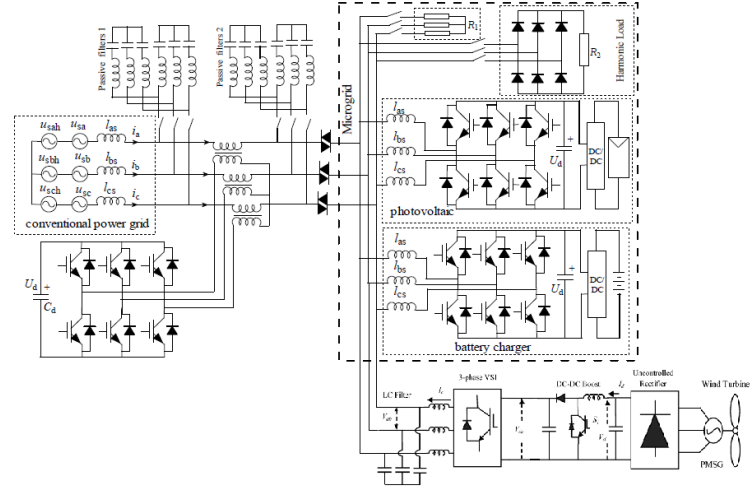


Fig. 8. Circuit model of the integrated power quality controller for solar wind integrated system

3.2. Power Flow control

When the power flow control & fault current limiter is concerned, solely the fundamental is taken under consideration. / Figure 9.

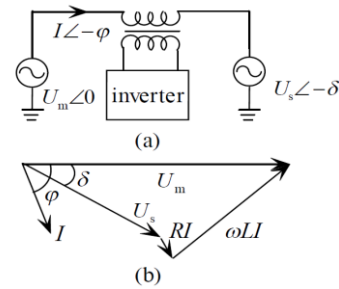


Fig. 9. Power flow control principle and its vector diagram

In terms of the above analysis, the primary winding projects adjustable impedance $Z_1 + (1-\alpha)Z_m$. With the change of coefficient α , the equivalent impedance of the primary winding will be achieved, that is shown in TABLE I. Therefore, once the primary winding is joined in series in circuit, it is applied to control the power flow between the traditional power utility and the microgrid or the inner power flow of microgrid. The schematic diagram of power flow manage is displayed in Fig.9 when the variable reactor is coupled in series between the sending and receiving ends. Suppose the equivalent impedance $Z_1 + (1-\alpha)Z_m$ of the variable reactor is $R+jX$. In terms of the vector diagram of Fig.9, the subsequent equations will be obtained.

$$U_m \cos \phi = U_s \cos(\phi - \delta) + RI \quad (21)$$

$$U_m \sin \phi = U_s \sin(\phi - \delta) + XI \quad (22)$$

Multiply $\cos \delta$ in either side of (21) and multiply $\sin \delta$ in either side of (22), then the subsequent equation is obtained by adding them.

$$U_m(U_m - U_s \cos \delta) = PR + QX \quad (23)$$

Multiply $\sin \delta$ in either side of (21) and multiply $\cos \delta$ in either side of (22), then the subsequent equation is obtained by subtracting them.

$$U_s \sin \delta = PX - QR \quad (24)$$

In term of (23)-(24), the active power and reactive power from U_m to U_s are

$$P = \frac{U_m}{R^2 + X^2} [R(U_m - U_s \cos \delta) + XU_s \sin \delta] \quad (25)$$

$$Q = \frac{U_m}{R^2 + X^2} [-RU_s \sin \delta + X(U_m - U_s \cos \delta)] \quad (26)$$

In the power system with high voltage level, the inductive reactance element of the line is much more than the resistance element of the line, (25)-(26) become

$$P = \frac{U_s U_m}{X} \sin \delta \quad \& \quad Q = \frac{U_m}{X} (U_m - U_s \cos \delta) \quad (27)$$

In microgrid with low voltage level, when the resistance element of the line is much more than the inductive reactance element of the line, the (25)-(26) is expressed as

$$P = \frac{U_m}{R} (U_m - U_s \cos \delta) \quad \& \quad Q = -\frac{U_m U_s}{R} \sin \delta \quad (28)$$

In terms of (28), there's a striking difference in power flow control, voltage regulation between the microgrid and traditional power system.[1]

3.3. Fault Current Limiter

When the terminal AX is interconnected in series in the circuit, in the normal operation state, the coefficient α is controlled as $\alpha = 1 + Z_1/Z_m$, the equivalent impedance of the primary winding AX is zero. Hence, the series transformer doesn't have any influence on the power system normal operation. the maximum system current I_{smax} of three phases is obtained by a current detecting circuit and compared with a reference current. If short-circuit fault occurs, maximum system current I_{smax} reaches the reference current, the coefficient α is controlled between -1 and 1 in the need of fault current, equivalent electrical resistance of the first winding AX is controlled between $Z_1 + Z_m$ and Z_1 therefore as to limit the system current to the specified value.

3.4. Voltage Compensation

In order to balance the voltage fluctuation, the primary winding of the transformer is connected in series between the power electric utility and load. when the load voltage is greater than the specified voltage, the coefficient α is controlled between zero and $1 + Z_1/Z_m$, the primary winding exhibits inductive impedance. The coefficient α is controlled greater than

$1 + Z_1/Z_m$ when the load voltage is lower than the required voltage, capacitive impedance is exhibited by the primary winding. therefore the load voltage is restrained by a stable voltage.

3.5. Harmonic Isolation

The above qualities of power flow control, fault current limiter and voltage compensation deals with the fundamental. If there exists harmonic within the power utility, the primary current contains nth order harmonic currents & the fundamental current, that's to mention, $i_1 = i_1^{(1)} + \sum i_1^{(n)}$. the fundamental element $i_1^{(1)}$ rather than harmonic is detected from the primary winding current i_1 and function as a reference signal. A voltage source inverter is applied to trace the reference signal $i_1^{(1)}$ so as to develop a fundamental compensation current $i_2^{(1)}$, that has a similar frequency as $i_1^{(1)}$. $i_2^{(1)}$ is reciprocally in phase injected to the secondary winding ax. when $\alpha = 1 + Z_1/Z_m$, the fundamental equivalent impedance of primary winding AX is zero, that is displayed in Fig. 10. Meanwhile, for the nth order harmonic, since solely a fundamental current is injected to the secondary winding of the transformer, i_2 doesn't consists of any order harmonic current other than the fundamental current, which means the transformer is open circuit to harmonic current. Therefore, the equivalent circuit of the transformer to the nth order harmonic is shown in Fig. 11. Then harmonic equivalent impedance of the transformer. From primary winding, the series transformer exhibits terribly low impedance at the basic and simultaneously exhibits a high impedance to harmonics so as to act as a "harmonic isolator". And then, the harmonic currents are forced to flow into the passive LC filter branches on either side.[1]

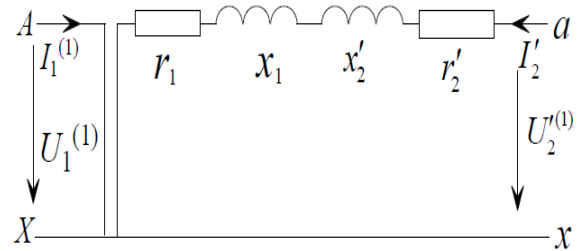


Fig. 10. Fundamental equivalent circuit

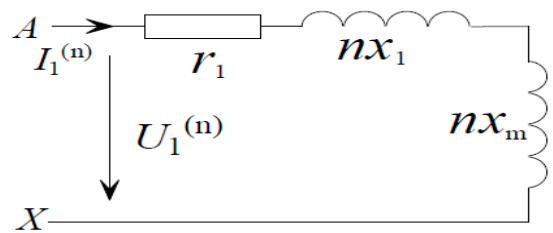


Fig. 11. Harmonic equivalent circuit

3.6. Integrated Power Quality Controller

When integrating the functions of the variable reactor, power flow control, , harmonic isolation,

voltage compensation, and fault current limiter an integrated power quality controller is achieved . For fundamental and harmonic, the primary winding of the series transformer exhibits the impedance of $Z_1^{(1)} + (1-\alpha)Z_m^{(1)}$ and $nZ_m^{(1)}$, respectively. that's to say, the primary winding of the series transformer exhibits adjustable impedance, that plays the role of power flow management, voltage compensation and fault current limiter to fundamental. Meanwhile, high impedance is exhibited by the primary winding of the series transformer exhibits $Z_m^{(1)}$ n to harmonic which can improve greatly the source impedance to harmonics really acts as a "harmonic isolator". Therefore, it will mitigate the harmonic high penetration.

4.SIMULATION RESULTS

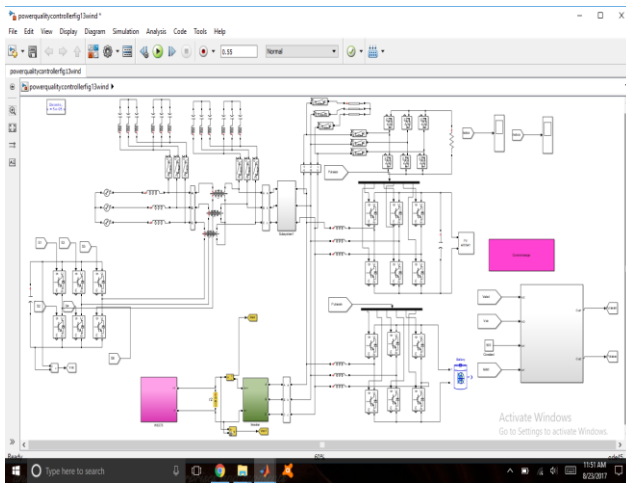


Fig. Simulation Diagram For The Main System

4.1 Verification of Variable Reactor

To begin with, the series transformer's turns ratio is 1:1, magnetizing impedance Z_m is 16.309 O, leakage impedance Z_1 is equal to 0.088O. The system voltage is 172V the principle circuit of the variable reactor is established by simplifying the Fig.8, which is shown in Fig.12. Z_1 and Z_2 are used as experimental loads. $Z_1 = 3.787 + j0.232\Omega$ and $Z_2 = 1.583 + j0.097\Omega$. Switch K_1 always keeps with open circuit in the verification experiment of variable reactor. The transformer's secondary winding current is adjusted continuously. Suppose a changes between -1 and 1, the measured voltage across U_{AX} and the primary winding's measured current I_1 is observed, so the equivalent impedance of the primary winding can be calculated accordingly, the calculated equivalent Z_{AX} on the base of observation impedance is almost equal to $Z_1 + (1-\alpha)Z_m$, which prove the validity of the principle of the transformer based on the magnetic flux controllable.

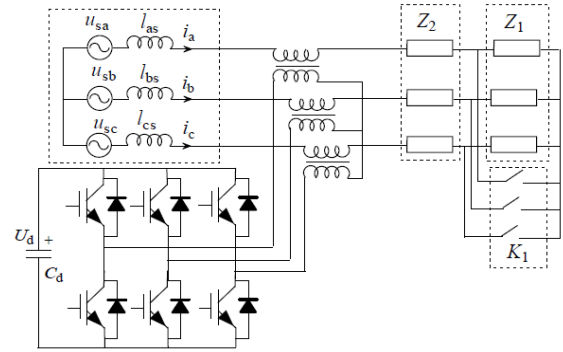


Fig. 12. Principle circuit of variable reactor

Fig.13 and Fig.14 record the transient current waveforms of primary winding when the injected primary currents change suddenly. Fig.13 shows current waveforms of primary winding when a suddenly changes from 0.6 to 0.1. Fig.14 shows current waveforms of primary winding once a suddenly changes from 0.1 to 0.6.[1] The above current waveforms imply the transformer with magnetic flux controllable own excellent transition characteristic. The characteristic are terribly valuable within the application of FACTS controllers

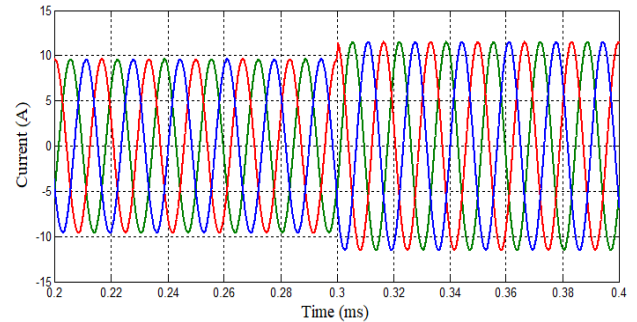


Fig. 13. Current waveforms of primary winding once α suddenly changes from 0.1 to 0.6

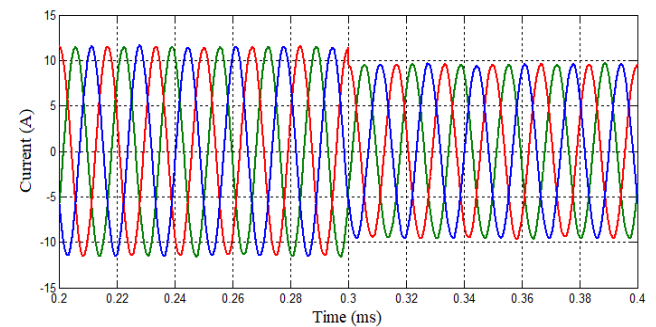


Fig. 14. Current waveforms of primary winding once α suddenly changes from 0.6 to 0.1

4.2 Verification of Fault Current Limiter

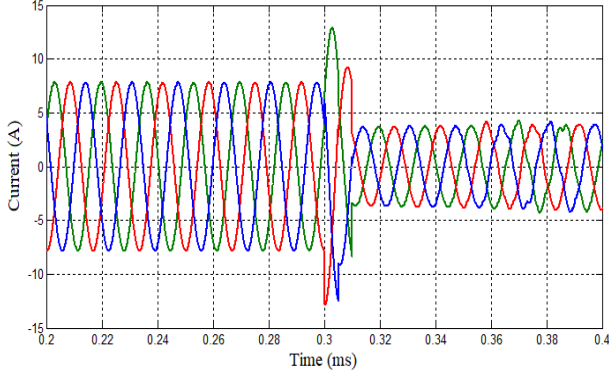


Fig. 15. Current waveforms of fault current limiter

In Fig.12, Switch K1 is employed for producing a fault. once the switch K1 is turned on, i.e., the resistor Z1 is short-circuited, the system current will increase greatly. A current detecting circuit is practiced to get the maximum system current I_{smax} of three phases. I_{smax} is employed to compare with a reference current. when it reaches the reference current, the compensation coefficient a is adjusted to 0, namely, the secondary winding of the transformer is open. The magnetizing impedance is exhibited by the primary winding therefore as to limit the system current. Fig.15 shows the current waveforms of the variable reactor when it works in the condition of fault current limiter. The system current is 18.23A when the system normally operates. At time T1, the fault happens, the system current increase rapidly. when a maximum current of a particular phase reaches 60A, which is assumed to happen at time T2, the compensation coefficient a is adjusted to 0, the system is restricted to 6.08A.

4.3 Verification of Harmonic High Penetration Mitigation and Filtering

The verification of the function of harmonic high penetration mitigation of the integrated power quality controller, the experiments are made in two conditions:

- 1) The voltages or currents at power supply side contain harmonics.
- 2) The voltages or currents at Micro grid side contain harmonics

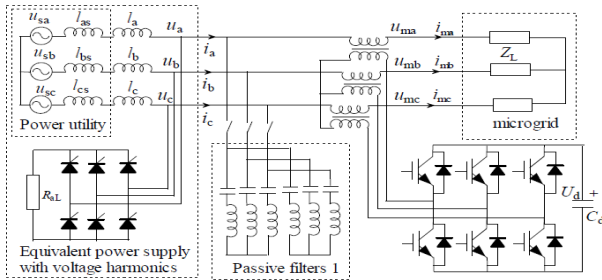


Fig. 16. circuit diagram for harmonic isolation in the initial condition

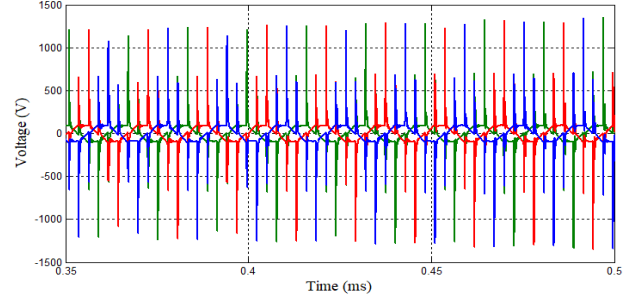


Fig. 17. System voltage waveforms when the IPQC is not applied

The circuit in the initial condition is shown in Fig.16. A three-phase resistor Z_L is employed to substitute the microgrid. A harmonic source is linked in parallel with the power system and a three-phase additional reactor indicated by l_a , l_b and l_c with the inductance of 2.51mH is united in series with power system at power supply side for providing the equivalent power utility background harmonics. Figs.17 and 18 show the waveforms of the system voltages u_a , u_b and u_c and currents i_a , i_b and i_c when the integrated power quality controller and Passive filter 1 aren't applied. During this case, the currents i_{ma} , i_{mb} and i_{mc} at microgrid side, namely, the system currents i_a , i_b and i_c , will also contain the same harmonic due to the system current. when the integrated power quality controller and Passive filter 1 ($C_3=40\mu F$, $L_3=28.17mH$, $C_5=20\mu F$, $L_5=20.28mH$) are applied, the current waveforms of i_{ma} , i_{mb} , i_{mc} at microgrid side is displayed in Fig.19. The voltage u_{ma} , u_{mb} and u_{mc} at microgrid side are almost like i_{ma} , i_{mb} and i_{mc} for resistor Z_L are linear. The DC voltage of DC capacitor (its capacitance and nominal voltage are 2200 μF and 400V) is about 150V.

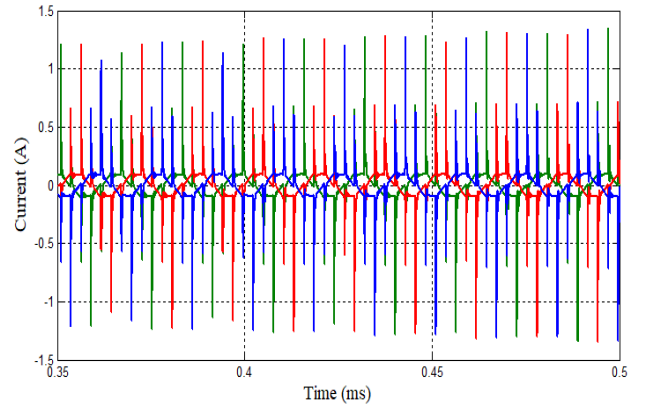


Fig. 18. System current waveforms when the IPQC is not applied

As to verify the harmonic isolation of the IPQC, the system voltage in Fig.17, the system current in Fig.18 and the current i_{ma} at microgrid side in Fig.19 of

phase-a are analyzed into Fourier series. The thd of the current i_{ma} is 2.73%.

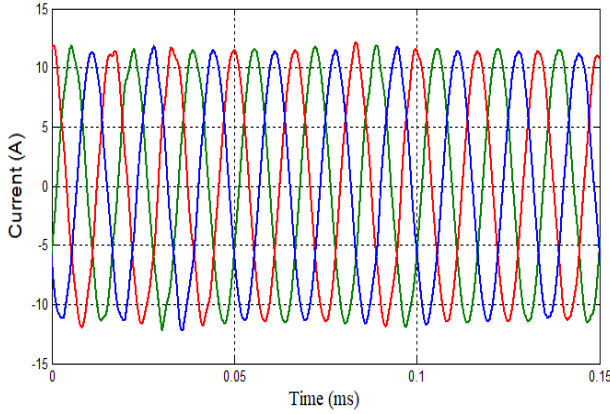


Fig. 19. Current waveforms at microgrid side when the IPQC is applied

The circuit in the second condition is shown in Fig.20. A harmonic-generating load is employed to substitute the microgrid. during this case, the system voltage is approximately sinusoidal. Figs.21 and 22 show the system voltage & current waveforms when the IPQC and Passive filter two are not used. when the integrated power quality controller and Passive filter two ($C3=40\mu F$, $L3=28.17mH$, $C5=20\mu F$, $L5=20.28mH$) are used, the system currents i_a , i_b and i_c waveforms at power utility side are shown in Fig.23. Likewise, the system voltage in Fig.21, the system current in Fig.22 and the system current in Fig.23 of phase-a are analyzed into Fourier series. The thd of System current i_a at power utility side is 0.21% when the IPQC and Passive filter 2 are used.

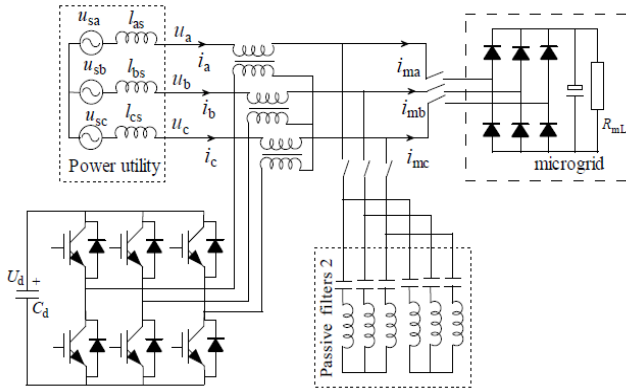


Fig. 20. circuit diagram for harmonic isolation in the second condition

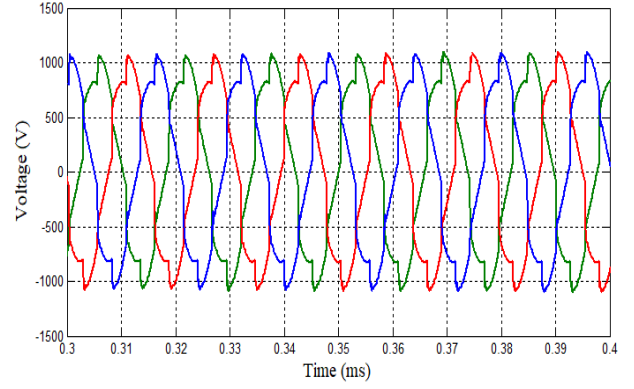


Fig. 21. System voltage waveforms when the IPQC is not employed

In terms of the results in two conditions, the IPQC performs in isolating harmonic. It can isolate both the harmonic from the power utility and the harmonic from microgrid. The harmonic currents are enforced to flow through the passive LC filter branches on either side. Therefore, IPQC will moderate the harmonic high penetration.

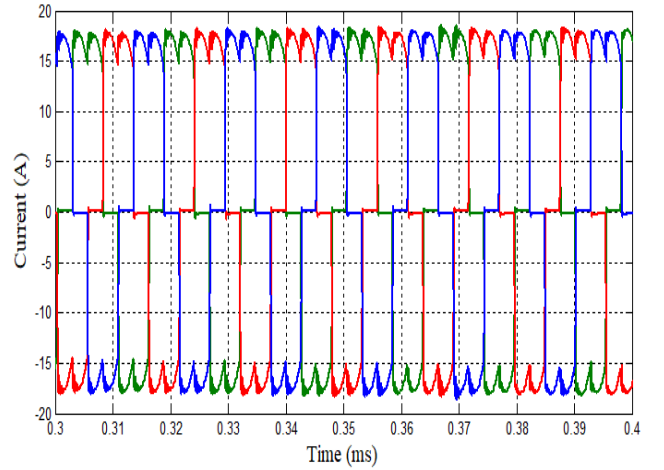


Fig. 22. System current waveforms when the IPQC is not employed

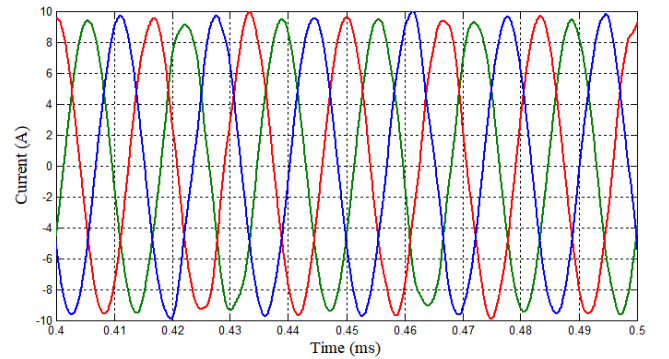


Fig. 23. System current waveforms when the IPQC is used

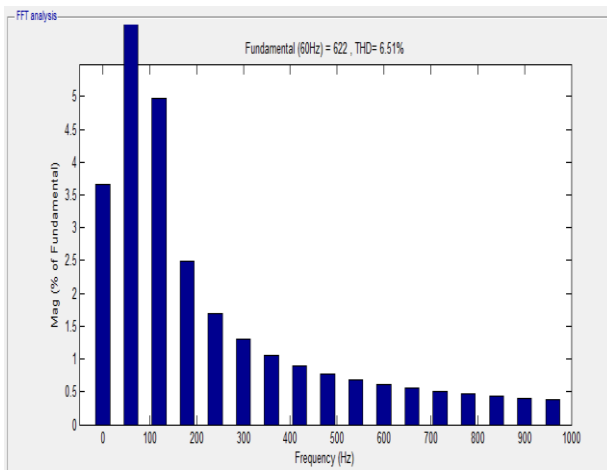


Fig. 24. THD of the system when IPQC is not connected

THD of the system when IPQC is not connected THD is calculated by practising FFT analysis in MATLAB/simulink and is shown as displayed in Fig 24 with 6.51% when IPQC is not connected.

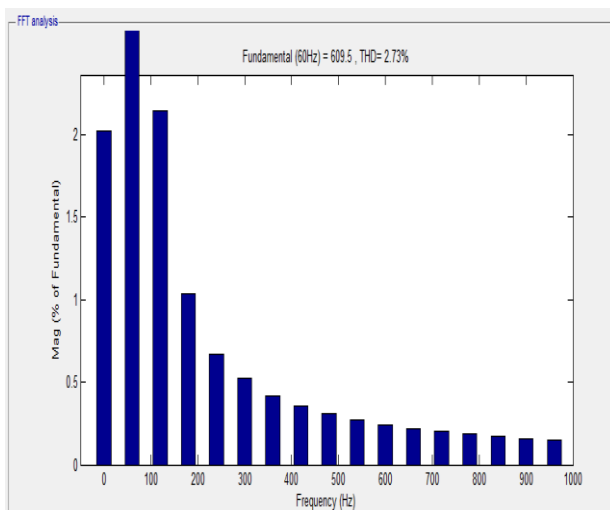


Fig. 25. THD of the system when IPQC is connected

Table 2. THD Comparison With & Without Integrated Power Quality Controller

SOURCE/ CONDITION	Without IPQC	With IPQC
Solar& wind	6.51	2.73

Table 2 shows the comparison of total harmonic distortion of the integrated PV wind system. THD of the system without integrated power quality controller is 6.51% and when IPQC is connected THD is reduced to 2.73%.

5. CONCLUSION

Microgrid with PV and wind is designed. Due to the integration of PV-wind to the grid many power quality issues have arisen. To overcome these problems an integrated Power Quality Controller (IPQC) is analyzed & designed. Power quality is improved by using IPQC with magnetic flux control based variable reactor. This variable reactor has the features of minimizing harmonics, simple control mechanism and adjustable impedance. Power flow control, fault current limiter and voltage compensation to fundamental are achieved by the adjustable impedance that is exhibited by primary winding. Meanwhile, the primary winding acts as a "harmonic isolator" by exhibiting high impedance to harmonics that can improve greatly the source impedance. Therefore, it mitigates harmonic high penetration. Power quality has been improved by reducing Total Harmonic Distortion (THD) using IPQC. Simulation results are verified by using MATLAB/simulink.

References

- [1] Li, Dayi, Z. Q. Zhu. "A novel integrated power quality controller for microgrid." *IEEE Transactions on Industrial Electronics* 62.5 (2015): 2848-2858.
- [2] Rahul Kozhi, Meeni Kumari L.Ramesh. "Simulation study of renewable energy driven microgrid," *Journal of Electrical Engineering*, Vol.15, Edition 1, Article 15.1.11, 2015.
- [3] R. H. Lasseter, A. Akhil, C. Marnay, et al. "Integration of distributed energy resources: the CERTS microgrid concept," USA: Consortium for Electric Reliability Technology Solutions, 2002.
- [4] C. Marnay, O. Bailey. "The CERTS Microgrid and the Future of the Macrogrid," LBNL-55281. August 2004
- [5] N. Hatziargyriou, H. Asano, R. Iravani, C. Marnay. "Microgrids," *IEEE Power and Energy Magazine*, vol.5, no.4, pp. 78-94, July/Aug. 2007
- [6] H. Akagi, E. H. Watanabe, M. Aredes. "Instantaneous Power Theory and Applications to Power Conditioning," *IEEE Press*, 2007, pp. 1-17
- [7] C. Sankaran. "Power quality." Boca Raton : CRC Press, 2002, pp. 133-146
- [8] R. C. Dugan. "Electrical power systems quality," New York : McGraw-Hill, 2003, pp. 167-223
- [9] B. Singh, K. Al-Haddad, A. Chandra. "A Review of active filters for power quality improvement," *IEEE Trans. Ind. Electron.*, vol.46, no.5, pp. 960-971, Oct. 1999

- [10] F. Z. Peng. "Application issues of active power filters," *IEEE Industry Application Magazine*, 21-30, Sep./Oct. 1998
- [11] S. Buso, L. Malesani, P. Mattavelli. "Comparison of current control techniques for active filter applications," *IEEE Trans. Ind. Electron.*, Vol. 45, pp. 722-729, Oct. 1998.
- [12] Y. Kusuma Latha, Ch. Saibabu, Y P Obulesu. "Unified Power Quality Conditioner for voltage sag and harmonic mitigation of nonlinear loads," *International Journal of Power Electronics and Drive Systems*, 2011;1(1):65-74 DOI 10.11591/ijpeds.v1i1.35
- [13] Y. Li, M. Vilathgamuwa, P. C. Loh. "Microgrid power quality enhancement using a three-phase four-wire grid-interfacing compensator," *IEEE Trans. Ind. Appl.*, vol. 41, no.6, pp. 1707-1719, Nov/Dec 2005
- [14] D. Menniti, A. Burgio, A. Pinnarelli, N. Sorrentino. "Grid-interfacing active power filters to improve the power quality in a microgrid," *13th International Conference on Harmonics and Quality of Power*, pp. 1-6, 2008
- [15] Paul C. Krause, Oleg Wasynczuk, Scott D. Sudhoff, John Wiley & Sons. "Analysis of electric machinery and drive systems," Inc, pp. 1-11, 2002
- [16] N. G. Hingorani, L. Gyugyi. *Understanding FACTS: Concepts and Technology of Flexible AC Transmission Systems*, IEEE Press, 2000, pp. 1-29
- [17] F. Blaabjerg, R. Teodorescu, M. Liserre, A.V. Timbus. "Overview of Control and Grid Synchronization for Distributed Power Generation Systems," *IEEE Trans. Ind. Electron.*, vol. 53, no. 5, pp. 1398-1409, Oct 2006.
- [18] R. Majumder, A. Ghosh, G. Ledwich, and F. Zare. "Power management and power flow control with back-to-back converters in a utility connected microgrid," *IEEE Trans. Power Syst.*, vol. 25, no. 2, pp. 821-834, May 2010.
- [19] M. Prodanovic, T.C Green. "High-quality power generation through distributed control of a power park microgrid," *IEEE Trans. Ind. Electron.*, vol.53, no.5, pp. 1471-1482, 2006
- [20] F. Wang, J. L. Duarte, M. A. M. Hendrix. "Grid-interfacing converter systems with enhanced voltage quality for microgrid application—concept and implementation," *IEEE Trans. Power Electron.*, vol.26, no.12, pp. 3501-3513, 2011
- [21] Kodanda Ram R B P U S B, Venu Gopala Rao Mannam. "Operation and Control of Grid Connected Hybrid AC/DC Microgrid using various RES," *International Journal of Power Electronics and Drive Systems*, 2014;5(2):195-202 DOI 10.11591/ijpeds.v5i2.6188
- [22] M. Azizi, A. Fatemi, M. Mohamadian, A.Y.Varjani. "Integrated solution for microgrid power quality assurance," *IEEE Transactions on Energy Conversion*, vol.27, no.4, pp. 992-1001, 2012
- [23] T. Ghanbari, E. Farjah. "Unidirectional fault current limiter: an efficient interface between the microgrid and main network," *IEEE Trans. Power Systems*, vol.28, no.2, pp. 1591-1598, 2013
- [24] A. H. Etemadi, R. Iravani. "Overcurrent and overload protection of directly voltage-controlled distributed resources in a microgrid," *IEEE Trans. Ind. Electron.*, vol. 60, no. 12, pp. 5629-5638, Dec 2013.
- [25] H. Rudnick, J. Dixon, L. Moran. "Delivering clean and pure power," *IEEE Power and Energy Magazine*, Vol.1, pp. 32-40, Sep./Oct. 2003 no.4, pp. 1263-1270, Apr. 2013
- [26] Seung-Ki Sul. "Control of Electric Machine Drive Systems," John Wiley & Sons, Inc, pp. 154-215, 2011
- [27] J. He, Y. Li, F. Blaabjerg. "Flexible Microgrid Power Quality Enhancement Using Adaptive Hybrid Voltage and Current Controller," *IEEE Trans. Ind. Electron.*, vol.61, no.6, pp: 2784-2794, June 2014.
- [28] R. Majumder. "Reactive power compensation in single-phase operation of microgrid," *IEEE Trans. Ind. Electron.*, vol. 60, no.4, pp. 1403 – 1416, April 2013